ROYAL SOCIETY OF CHEMISTRY

Photochemical & Photobiological Sciences

Modulation of the carboxamidine redox potential through photoinduced spiropyran or fulgimide isomerization.

Photochemical & Photobiological Sciences

Modulation of the carboxamidine redox potential through photoinduced spiropyran or fulgimide isomerization.

M. Crawford Andrews,[a] Ping Peng,[ab] Amit Rajput,[ad] Anthony F. Cozzolino*[a]

Carboxamidines functionalized with either a spiropyran or fulgimides photoswitch were prepared on multigram scales. The thermal, electrochemical, and photochemical ring isomerizations of these compounds were studied and the results compared with related systems. The photochemical isomerizations were found to be reversible and could be followed by ^{1}H NMR and UV-vis spectroscopy. The spiropyran/merocyanine couple was thermally active and an activation enthalpy of 116 kJ/mol was measured for ring-opening. These measurements yielded an enthalpy difference of 25 kJ/mol between the open and closed states which is consistent with DFT calculations. DFT calculations predicted a charge transfer to the carboxamidine group upon ring closure in the fulgimide and a charge transfer from the carboxamidine group upon switching the spiropyran to the merocyanine form. This was confirmed experimentally by monitoring the change in the oxidation potential assigned to the carboxamidine group. The potential of these molecules to therefore act as a new class of photoresponsive ligands that can modulate the ligand field of a complex is discussed.

Introduction

Stimulus-responsive molecules show promise in many fields, including data storage,[1,2] drug-delivery,[3,4] detection,[5] and catalysis.[6,7] Light is a particularly attractive stimulus because it can be easily tuned and varied, the stimulus can be applied instantaneously, and there are no by-products associated with it. Light has been used to produce chemical changes in a variety of ways, such as the oxidation of water or organic compounds by producing hydroxyl radicals over TiO_2[8–10] or the reduction of water to produce H_2 facilitated by $[Ru(bpy)_3]^{2+}$. In the $[Ru(bpy)_3]^{2+}$ complex, the ligands play a crucial role in the reduction of water, as this complex must undergo metal-to-ligand charge transfer in order for the reaction to take place.[11] Alternatively, photoswitchable molecules can be used to affect the ligand field. Certain photoswitchable molecules undergo a concomitant isomerisation and change in π-framework upon irradiation. This, in turn, can affect the electronic structure of a pendant ligating group.[12–14] Photoswitchable moieties have been used in combination with neutral σ-donor/π-acceptor ligating groups, particularly, N-heterocyclic carbenes (NHC)[15–17] and 1,10-phenanthrolines.[18–23] Fig. 1 illustrates some examples where the photoswitchable ligand induces a measurable change in the ligand field. Fig. 1a illustrates the first example of a photoswitchable ligand, 4-styrylpyridine, being used to induce a change in spin state at the metal. Here, the change in the ligand field was too small for the effect to be observed at room temperature.[24] Fig. 1b illustrates a more recent example where photoisomerisation of a diarylethene derivatised ligand induces room temperature spin-crossover.[23] Fig. 1c shows a system where the changes in the carbonyl stretches are observed as a as a function of irradiation induced switching.[18] Fig. 1d illustrates the use of a photoswitchable carbene ligand on rhodium that modifies the rate of hydroboration upon irradiation.[16] Earlier studies on this ligand measured a change in the Tolman electronic parameter (TEP) upon switching of 6 cm^{-1}, which is equivalent to the change in donating ability from that of a carbene to that of some phosphines.[15] Key to these advances is the ability of the photoinduced isomerization to push or pull electron density to or from the ligating group. The more pronounced the effect, the larger the response in the complex.

a. Department of Chemistry and Biochemistry, Texas Tech University, MS 41061, Lubbock, TX 79409, USA, Fax: 001 806 742 1289; Tel: 001 806 834 1832; E-mail: anthony.f.cozzolino@ttu.edu

b. Current Address: State Key Laboratory of Materials Processing and Die & Mold Technology, School of Materials Science and Engineering, Huazhong University of Science and Technology, 1037 Luoyu Road, Wuhan 730074, P. R. China

c. Department of Basic and Applied Science, School of Engineering, G.D. Goenka University, Sohna Road, Gurgaon 122103, Haryana, India, Tel: +91-7300681852
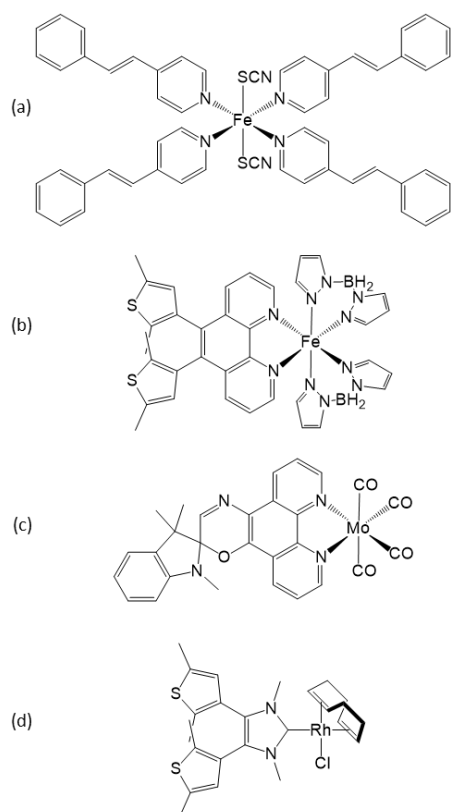
Fig. 1. Notable examples of complexes with photoswitchable ligands that have measurable effects on the ligand field.[16,18,22,24]

Despite these exciting possibilities in the use of photochromic molecules to modulate the ligand field, most studies focus on varying pendant groups to modify the switching behaviour, rather than vice versa. As such, the degree to which a photoswitch can affect the electronic properties of a pendant group is not well established. In this study, carboxamidines (Fig. 2a) were chosen as a pendant group around which to incorporate the photoswitches because they are well established as ligands in the field of coordination chemistry, they have not been explored as a pendant group on photoswitches, and they provide up to three opportunities to tune the molecule. The amidine moiety (Fig. 2a, blue) can support the photoswitchable moiety at either the amine or imine nitrogen (yellow and red, respectively). By varying substitutions at the other nitrogen, control can be exerted over solubility, sterics, and electronics.[25,26] Variations at R_3 (green) allow tuning of the bite angle, solubility and electronic structure. The photoswitchable moieties that we chose to start with are fulgimides (Fig. 2b) and spiropyrans (Fig. 2c). Upon irradiation with UV-light they undergo a ring-closing or -opening. These events are accompanied by colour changes that are readily followed by UV–vis spectroscopy.[27,28]
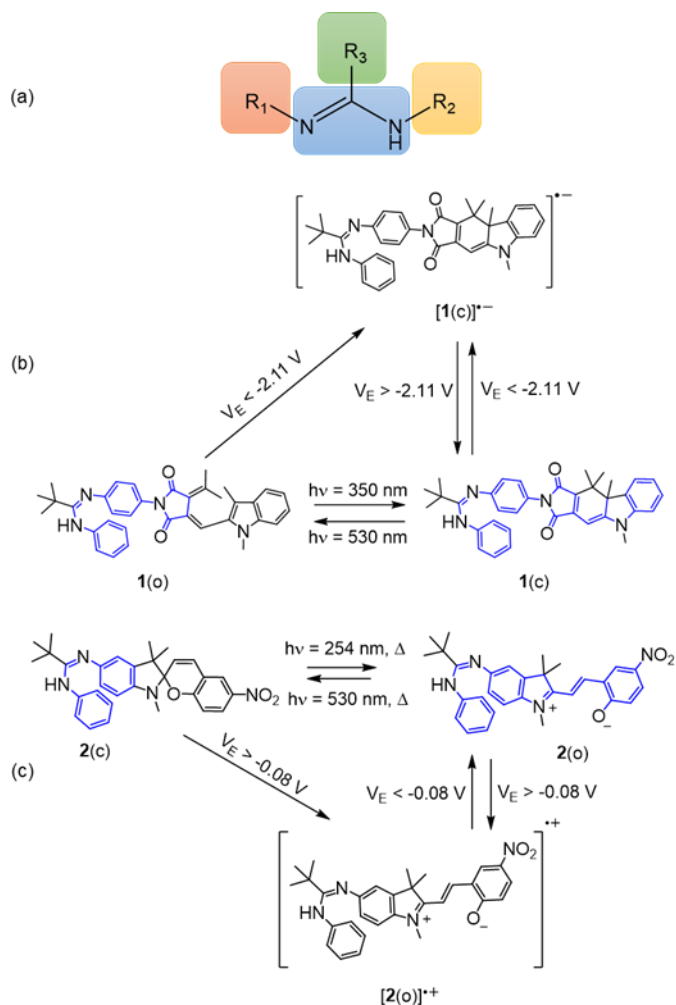

Fig. 2. (a) Generic carboxamidine and graphical summaries of experimentally determined photochemical and electrochemical pathways staring from (b) **1**(o) and (c) **2**(c).

Herein we present the synthesis of two new photoswitchable molecules, one incorporating a fulgimide (**1**) and the other incorporating a spiropyran (**2**). Structures were elucidated by IR and NMR spectroscopies and supplemented with density functional theory (DFT) calculations. Photophysical and electronic properties and structural changes upon irradiation and subsequent photoisomerization were investigated by absorption spectroscopy (UV–vis), cyclic voltammetry (CV), photoelectrochemistry, and spectroelectrochemistry. DFT calculations were also used to understand and supplement experimental results. Fig. 3 and 4 summarize the various photochemical, thermal, and electrochemical processes observed for **1** and **2**. The degree of charge-transfer to and from the carboxamidine is evaluated electrochemically by monitoring the oxidation potential of the carboxamidine as a function of irradiation. This is corroborated by DFT calculations.

Results and Discussion

Synthesis and structural characterisation

The target molecules and the photoswitched forms are shown in Fig. 2b and Fig. 2c Both photoswitches were prepared from the same imidoyl chloride precursor (Scheme 1).[29] The open form of compound **1**, **1**(o), and the closed form of **2**, **2**(c), were prepared according to Scheme 1 in multigram scales. This follows our strategy to design these molecules in such a way that the photoswitchable moiety electronically integrates with the carboxamidine group, while utilizing a minimal number of simple/scalable synthetic steps. For **1**(o), the *E*-isomer at the fulgimide (*E*$_{fulg}$) was selectively isolated by starting from the pure (3*E*)-3-[(1,3-dimethyl-1*H*-indol-2-yl)methylene]dihydro-4-(1-methylethylidene)-2,5-furandione.[30] Both molecules were characterised by high-resolution mass spectrometry and IR, ^{1}H and ^{13}C NMR spectroscopies.
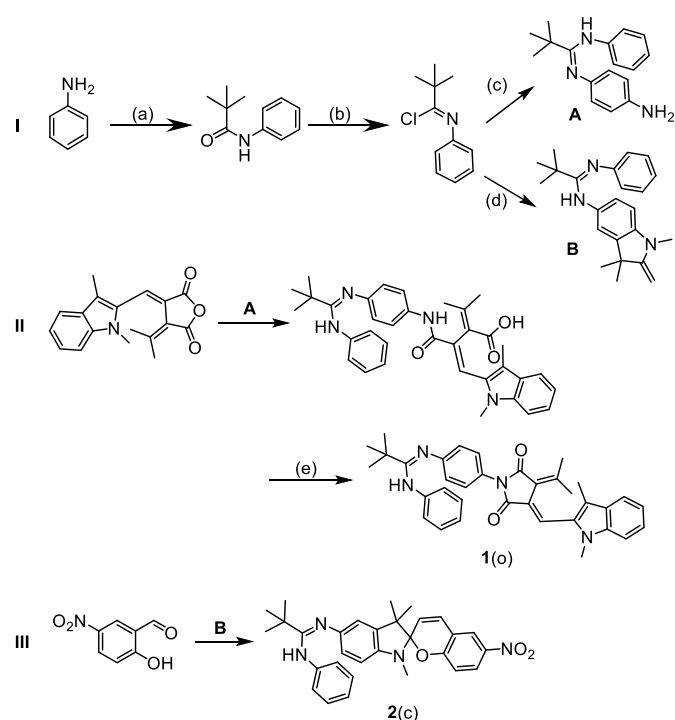
Scheme 1. Synthesis of **1**(o) and **2**(c). (a) pivaloyl chloride, Et$_3$N, DCM (b) PCl$_5$, DMF (c) (i) tert-butyl(4-aminophenyl)carbamate, Et$_3$N, toluene (ii) trifluoroacetic acid, DCM (d) 1,3,3-trimethyl-2-methyleneindolin-5-amine, Et$_3$N, THF (e) acetic anhydride, toluene.

Solid and Solution State Conformations

A crystal structure was determined for **1**(o); however, the quality was only sufficient to allow connectivity and configuration to be determined (Tables S3-S5). The crystal structure shows only the *E*$_{fulg}$-isomer which is consistent with the synthetic approach as well as the UV–vis absorption spectrum (the *Z*$_{fulg}$-isomer would be expected to absorb at longer wavelengths).[30] ^{1}H NMR spectra taken in d$_6$-DMSO show that irradiation with UV light (350 nm) results only in **1**(c) as no peaks associated with either the *E*$_{fulg}$-isomer or the *Z*$_{fulg}$-isomer are observed (Fig. S7). Subsequent irradiation with green (530 nm) light leads only to the *E*$_{fulg}$-isomer of **1**(o).
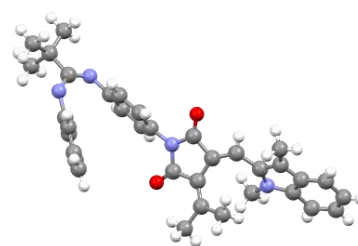
Fig. 3. Ball and stick representation of **1**(o) from low-quality single crystal data.

In this crystalline phase, the configuration in which the aryl groups are both trans- to the *t*-butyl group (Fig S47a) is observed. Furthermore, based on the markedly different bond lengths and deviations from planarity in the crystal structure, we can confidently assign the tautomer where the photoswitchable group is bound to the imine nitrogen of the carboxamidine (Fig. 4, boxed species). Because single crystals of **1**(c), **2**(c), and **2**(o) could not be isolated, DFT calculations were used to elucidate the relative energies of the different carboxamidine tautomers and configurations for each photoswitch in the gas phase. Several configurations were modelled (Table S6), but given the small differences in energy among most configurations, it is likely that all configurations are in dynamic equilibrium under experimental conditions, i.e., in solution at room temperature. In both tautomers, the *Z*-configuration is the lowest or nearly the lowest energy confirmation for **1** and **2**. We have chosen to use the *Z*-configuration of Tautomer 1 (boxed species in Fig. 4) for all subsequent calculations discussed herein for consistency, which is also consistent with the crystal structure of **1**(o).
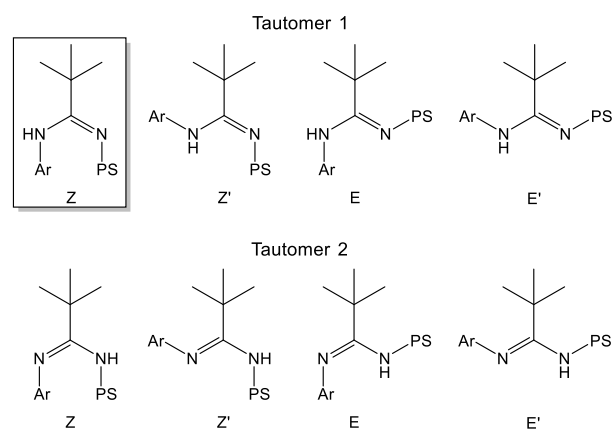
Fig. 4. Configurations of photoswitches around carboxamidine. "PS" represents the photoswitchable moiety.

Photochemical Behaviour

Functional groups are known to influence the switching behaviour of spiropyrans and fulgimides. It has been shown that electron donating groups on the indoline moiety of spiropyrans and electron withdrawing groups on the opposing phenyl ring result in a photostationary state that strongly favours one isomer while electron donating groups on the indoline moiety can influence the rate of thermal isomerisation to the point in

which it competes with (or dominates over) the photochemical processes.[31–34] Recent computational studies show that the photocolouration of spiropyrans with an acceptor group on the pyran ring (refer to compound **4** in Scheme 2) proceeds by a triplet state for both CO cleavage and cis/trans isomerization. The rate-determining step for both thermal and photocolouration is the subsequent *cis-trans* isomerisation.[35] In fulgides, the ability of functional groups to stabilize a highly zwiterionic excited state (charge transferred from the (hetero)aromatic group to the fulgide) plays a crucial role in the photochromism.[36] Sterics can influence the ratio of isomers that make up the photostationary state of fulgides.[37] Substituents also affect the absorption spectra of both spiropyrans[31] and fulgimides, and therefore the wavelengths that lead to photoswtiching.[27,38,39] We wanted to determine how the introduction of the carboxamidine functional group to the photoswitchable portion of the molecule would affect the photoswitchable behaviour. Furthermore, we wanted to probe the effect of switching on the carboxamidine group.

Depending on the concentration, solutions of **1**(o) and **2**(c) were colourless to pale yellow, and irradiation with a UV light source resulted in vibrant purple solutions. UV–vis spectra are shown in Fig. 5, and the relevant transitions are summarised in Tables S1 and S2. Upon irradiation of a methanol solution of **1** with 350 nm light, the peak at 368 nm diminishes as a peak at 531 nm grows in (Fig. 5, left). This is consistent with the behaviour of fulgimides upon ring-closing (**1**(o) to **1**(c)).[40] However, the substitution of the carboxamidine appears to have some effect on the relative energies of the frontier orbitals. The HOMO-LUMO transition (associated with the peak at 368 nm) of **1**(o) is higher in energy than similar unsubstituted fulgimides.[41–46] For instance, the structurally related fulgimide **3**(o) (Scheme 2) absorbs at 400 nm. [42] The HOMO-LUMO transition of **1**(c) (associated with the peak at 535 nm) is lower in energy than some fulgimides but nearly identical to that of **3**(c).[42] Solvatochromic effects could be responsible for the differences observed, but DFT calculations predict similar, albeit small (~0.06 eV), differences in orbital energies between the carboxamidine-substituted and unsubstituted fulgimides.

The spectra are consistent with the time-dependant DFT (TDDFT) calculated electronic transition energies and oscillator strengths shown in Table S1. The HOMO-LUMO transition of **1**(c) is lower in energy than the HOMO-LUMO transition of **1**(o), resulting in a red-shift in the peak of interest in the absorption spectrum. Relevant orbitals are shown in Fig. 6. ^{1}H NMR was used to determine the speciation after irradiation. In d[6]-DMSO, quantitative conversion from **1**(o) to **1**(c) occurs upon UV-irradiation (350 nm) as seen in Fig. S7.
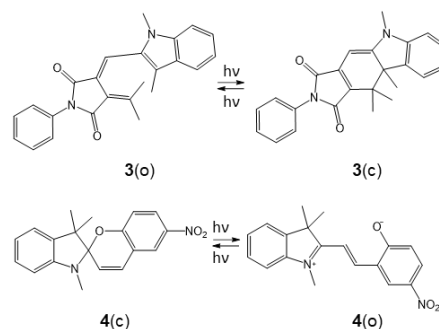
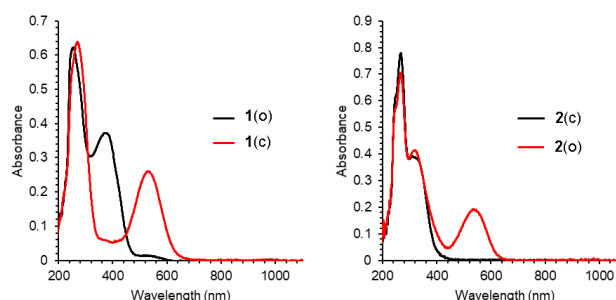**Scheme 2.** Unsubstituted fulgimide (**3**) and spiropyran (**4**).

Fig. 5. UV–vis spectrum of 25.0 µM fulgimide **1**(o) in methanol before and after 15 minutes irradiation at 350 nm to give **1**(c) (left) and 25.0 µM spiropyran **2**(c) in methanol before and after 15 minutes irradiation at 350 nm to give **2**(o) (right).
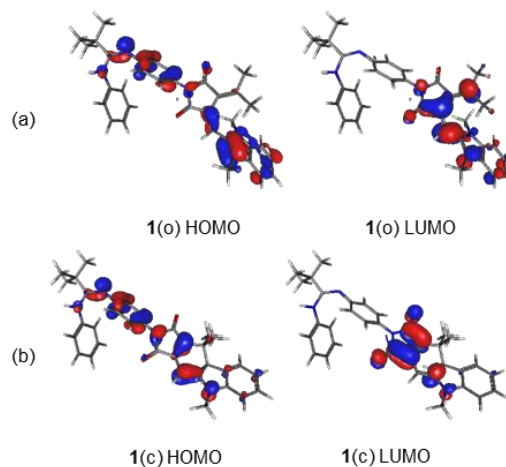

Fig. 6. Frontier orbitals of (a) **1**(o) and (b) **1**(c) (0.04 a.u. isosurfaces).

The absorption spectra of **2**(c) has a λ_{max} of 316 nm in methanol which is consistent with other donor-substituted nitro-spiropyrans. For instance, a methoxy group in place of the carboxamidine in **2**(c) has a λ_{max} of 315 nm in ethanol.[31] As **2**(c) isomerises to **2**(o) under UV irradiation (Fig. 5, right) a peak grows in at 537 nm which is consistent with the behaviour of nitro substituted spiropyrans with hydrogen or electron donor groups in the R position (Scheme 2, **4**).[31] No peak diminishes appreciably which is again consistent with the known isomerisations of spiropyrans to form merocyanines.[31] As depicted in Table S2, TDDFT calculations predict similar behaviour. The HOMO-LUMO transition of **2**(o) shifts to a higher

energy transition than that of **2**(c). Experimentally, no band is observed in this region for **2**(c). Upon irradiation, a new peak grows in as **2**(o) is formed. TDDFT suggests that the HOMO-LUMO transition for **2**(c) has a negligible oscillator strength (*f*) and is therefore not observed experimentally. This is likely because the HOMO is largely localised on the indoline side of the spiro-carbon while the LUMO is entirely localised on the other side of the spiro-carbon and these rings are orthogonal to each other (Fig. 7a). Upon opening, the HOMO and LUMO become coplanar (Fig. 7b) which renders this transition far more efficient than in the closed form leading to an observable absorption at 537 nm for **2**(o). The HOMO-LUMO transition (537 nm) of **2**(o) occurs at higher energy as compared to the related spiropyran **4**(o) (Scheme 2) that lacks the carboxamidine group.[47] This is consistent with TDDFT calculations which give an energy difference (transition of **2**(o)-transition of **4**(o)) of 0.05 eV. Fig. 7 illustrates a significant reorganisation of the electron density associated with the HOMO at the carboxamidine group. Upon switching of **2**, electron density appears to be pulled away from the carboxamidine as a result of electronically connecting the electron deficient nitro substituted ring to the rest of the molecule. This prompted us to probe for a measurable change in the electronic structure of the redox-active carboxamidine electrochemically (vide infra). It should be noted that absorption spectra were calculated without accounting for solvent effects. This may contribute to the differences in λ_{max} observed between the calculated and experimental spectra as shifts in the λ_{max} of up to 30 nm have been observed for related fulgides and fulgimides[30,48] and up to 100 nm for related spiropyrans depending on the solvent.[33,49]
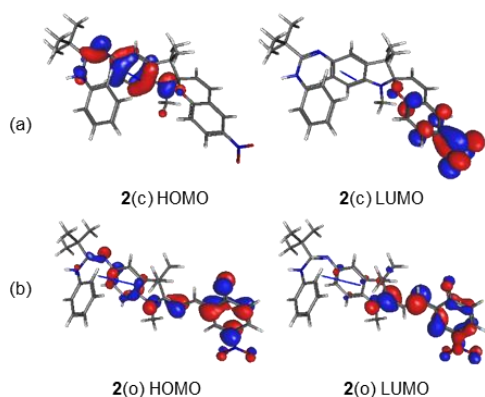

Fig. 7. (a) HOMO and LUMO of **2**(c) and (b) HOMO and LUMO of **2**(o) (0.04 a.u. isosurfaces).

Photochemical Stability

In order to determine how robust the photoswitchable behaviours of **1** and **2** are, solutions of the compounds were irradiated through ten cycles of UV and visible light. It was found that both compounds efficiently switched under a wide range of UV light (254, 350, and 378 nm in methanol). **1**(c) could be converted back to **1**(o) by irradiating with green light (530 nm). The left side of Fig. 8 shows the reversible photoswitchable behaviour of **1** by monitoring the absorbance at 531 nm during several cycles of alternating UV and visible light. Irradiation of

the spiropyran **2**(c) with 254 nm light led to ~25% **2**(o) as seen in Fig. 8 (right), red triangles, but resulted in decomposition upon repeated cycling. Irradiation of **2**(c) with 350 nm light resulted in a lower conversion (only ~11%) to **2**(o) which can also be seen in Fig. 8 (right). Irradiation at 419 nm or 530 nm could convert **2**(o) back to **2**(c) as depicted for ten cycles in Fig. 8 (right).
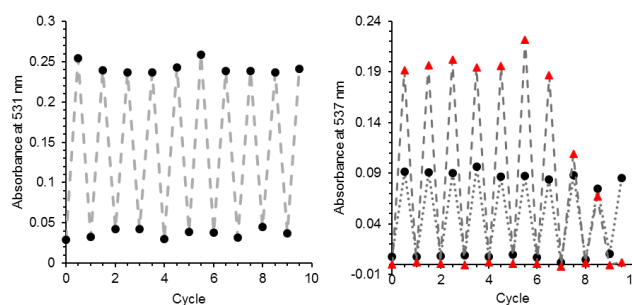

Fig. 8. Absorbance of a solution of **1**(o) (25.0 µM in methanol) measured at 531 nm before and after irradiation with 350 nm light, then alternating irradiation with 530 nm light and 350 nm light (left) and a solution of **2**(c) (25.0 µM in methanol) measured at 537 nm before and after irradiation with 350 nm light (black circle) or 254 nm light (red triangle) , then alternating irradiation with 530 nm light and UV light (right). Dashed lines are provided as a visual aid.

Thermochemical Behaviour

As **2** was found to thermally isomerise, the activation energy ($\Delta G^{\ddagger}$) for this was determined experimentally. The Eyring-Polanyi equation was used to plot (Fig. S16) the temperature dependence of the rate constant for the thermal conversion of **2**(c) to **2**(o), which followed first order kinetics in methanol and to determine the enthalpy ($\Delta H^{\ddagger}$ = 116 kJ·mol^{-1}) and entropy ($\Delta S^{\ddagger}$ = 0.04 kJ·K^{-1}·mol^{-1}) of activation. Literature values for related systems are on the order of 75-108 kJ·mol^{-1}, but may be affected by the solvent,[50] donor/acceptor groups[35] or presence of suitable nucleophiles.[51,52] This slightly higher activation energy is in line with the findings of Leszczynski who determined that systems with small bond length alternation (BLA) values, and therefore a greater contribution from the zwiterionic form of the merocyanine, had higher cis/trans isomerisation had a higher activation energy than the C-O cleavage and is the rate determining step.[35] The BLA value for **2**(o) is 0.004; lower than the calculated value for **4**(o) (BLA value = 0.019) which has an experimental activation energy for ring opening of 102 kJ/mol. The $\Delta H^{\ddagger}$ (90.7 kJ·mol^{-1}) and $\Delta S^{\ddagger}$ (-0.02 kJ·K^{-1}·mol^{-1}) for the reverse reaction were also determined. This gives a ΔH of 25.3 kJ mol^{-1} (Fig. 9) for the overall conversion of **2**(c) to **2**(o). This is consistent with DFT calculations, which give a ΔH of 22.8 kJ mol^{-1} for this conversion. The absorption spectra of **1**(o) and **1**(c) do not change as a function of time at accessible temperatures (Fig. S35 and S36), so it is not possible to experimentally determine an activation energy or change in enthalpy.
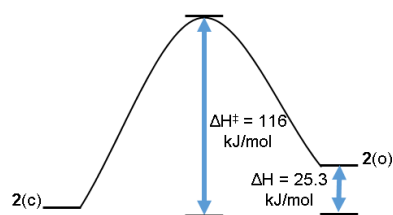
Fig. 9. Energy diagram for the thermal conversion of **2**(c) to **2**(o).

W = O, S
X = O, NPh, p-NO$_2$C$_6$H$_4$N, NCH$_2$CO$_2$H, NBz
Y = H, CH$_3$, adamantylidene
Z = CH$_3$, adamantylidene

Scheme 3. First examples of reversible electrocyclisation in fulgides.[55]

Electrochemical Behaviour

The carboxamidine moiety is known to be redox active.[53] If there is efficient electronic communication between this group and the photoswitch, then a change in the redox potential associated with the carboxamidine should be observed upon photoinduced isomerisation. Cyclic voltammetry (CV) was first performed on **5** (Fig. 10) to characterize the redox response of the carboxamidine group under these experimental conditions. Consistent with literature (1.24 V vs. Ag/AgCl[54]), the only redox response observed was an irreversible oxidative wave at 0.66 V vs. Fc/Fc$^+$ (Fig. S37). The CV of **1**(o) (Fig. 11, left) displays two redox processes: one oxidation at 0.67 V and one reduction at $E_{1/2}$ = −2.11 V. The oxidative response is irreversible and attributed to the carboxamidine group. The reductive response is quasi-reversible in nature (ΔE_p = 180 mV, i$_{pc}$/i$_{pa}$ ≈ 1) and consistent with the reductive responses of fulgides which have been shown to induce cyclisation as determine by Fox and Hurst (Scheme 3).[55] The voltammogram of an CH$_3$CN solution of **2**(c) (Fig. 11, right) shows three redox processes. There are two quasi-reversible oxidations at $E_{1/2}$ values of −0.08 V (ΔE_p = 180 mV) and 0.65 V (ΔE_p = 160 mV). The first oxidation is attributed to the oxidation of the indole nitrogen[56,57], and the latter is attributed to the carboxamidine group. There is one irreversible reduction at −1.72 V associated with the reduction of the nitro group.[57,58]
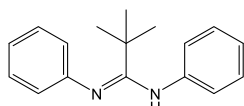

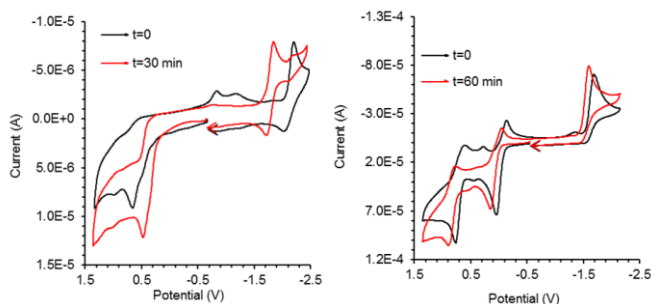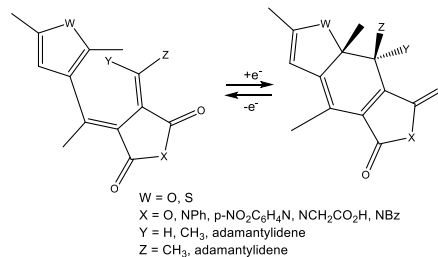**Fig. 10.** Diphenyl carboxamidine CV reference (**5**).

Fig. 11. CV (100 mV/s) of a 1.0 mM solution of **1**(o) (left) and **2**(c) (right) before and after UV-irradiation in CH$_3$CN (0.1 M in Bu$_4$NPF$_6$) at a platinum working electrode. Indicated peak potentials are in V vs. Fc/Fc$^+$. Time interval indicated is time of irradiation. Arrows indicate direction of scan.

Photoelectrochemistry

Given that the carboxamidine group is electrochemically active, photoelectrochemical experiments were performed to determine the extent to which the photoisomerisation would affect the oxidation potential of the carboxamidine group (oxidation event around 0.7 V) in **1**(o) and **2**(c). This would be an important measure of the ability of the photoswitch to influence the electronic structure of a ligating group and, ultimately, the ligand field in a manner analogous to redox switchable ligands.[59–62] Solutions of **1**(o) and **2**(c) were irradiated with 254 nm UV light at 30-minute intervals. After each 30-minute interval, a voltammogram was recorded. Photoisomerisation of **1**(o) to give **1**(c), results in a cathodic shift of the oxidative wave to 0.44 V and an anodic shift of the reductive wave to −1.81 V (Fig. 11, left, Table 1). This implies that the carboxamidine group of **1**(c) is easier to oxidize by 0.23 V and would therefore be a more reducing ligand if bound to a metal than the open form, **1**(o). This is consistent with the calculated change in the HOMO of **1**, where the closed form has a HOMO that is 0.19 eV less stable than the open form. For **2**(c) at t = 0, three redox responses were observed at 0.65, −0.08, and −1.72 V, respectively, but after 30 minutes of UV-irradiation to give **2**(o), the redox responses shifted anodically to 0.76, 0.01, and −1.62 V, respectively (Fig. 11, right, Table 1). Here, the implication is that the carboxamidine group of **2**(o) is harder to oxidize upon switching to **2**(o) as compared to **2**(c) and would therefore be a more oxidizing ligand if bound to a metal than the closed form. Since this is the second oxidative wave, the same analogy to the changes in the HOMO energy levels cannot be easily made. It should be noted that **2**(c) does not convert completely to **2**(o) upon UV-irradiation (vide supra). The observed redox responses are, therefore, a convolution of both **2**(c) and **2**(o) isomers.

Samples of **1**(c) and **2**(o) could be isolated. Irradiation of a dichloromethane solution of **2**(c) led to the precipitation of **2**(c). Scale-up allowed the precipitate to be isolated and it was characterised as pure by ^{1}H NMR. The removal of solvent from irradiated solutions of **1**(o) in DCM allowed for the isolation of pure **1**(c) as confirmed by ^{1}H NMR. CVs were recorded for the isolated switched forms (**1**(c) and **2**(o), Fig. S40 and S41 respectively) and found to be virtually identical to the CVs that were recorded when the compounds were irradiated in situ. The similar results from both experiments on **2**(o) are likely due to thermal equilibration that occurs upon dissolution.
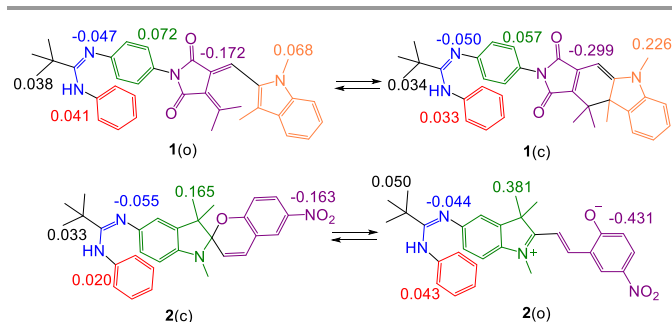
Fig. 12. Charge distribution from summed Hirshfeld charges for photoswitchable molecules. The colour designates group of atoms to which the charge corresponds.

Table 1. Redox potentials (V) of **1**(o) and **2**(c) before and after irradiation with 254 nm light for given time intervals. Calculations were done with B3LYP functional, TZV(d) basis set.

|	**1(o)**		
	E_{ox} of carboxamidine (V)	$E_{1/2ox}$ (V)	$E_{1/2red}$ (V)
t = 0	0.67		−2.11
t = 30 min	0.44		−1.81
Experimental E_{ox} of 1(c) − E_{ox} of 1(o)	−0.23		
Calculated* E_{HOMO} of 1(c) − E_{HOMO} of 1(o)	−0.19 eV		
	2(c)		
t = 0	0.65	−0.08	−1.72
t = 30 min	0.76	0.01	−1.62
t = 60 min	0.80	0.01	−1.63
Experimental $E_{1/2ox}$ of 2(o) − $E_{1/2ox}$ of 2(c)		0.09	
Calculated* E_{HOMO} of 2(o) − E_{HOMO} of 2(c)		0.05 eV	

To corroborate the idea of using the switching event to push or pull electron density from the carboxamidine group, the Hirshfeld charges were calculated and summed across various groups within each molecule to provide a measure of the overall change in electron density (or charge redistribution) upon switching. For **1**, a net increase in electron density was calculated for the carboxamidine group following ring closing, while a net decrease in electron density was calculated for the carboxamidine group in **2** upon ring opening (Fig. 12). These results are both consistent with the changes observed by CV. For both **1** and **2**, the implication is that the ligand field generated by the carboxamidine group could be modulated by affecting a cyclisation or ring opening event in a peripheral group. The extent to which this effect can be transferred onto a metal ion will be the subject of future investigations.

While running multiple voltammetric cycles on **1**(o) and **2**(c), it was observed that the quasi-reversible events shifted anodically

at slower scan rates. This is consistent with CV's of photoswitched molecules **1**(c) and **2**(o), respectively. Figs. S42-S48 show that for CV's of solutions of **1**(o) and **2**(c) at slower scan rates, the voltammograms begin to resemble those of the photoswitched forms.

Spectroelectrochemistry

Potentials were held constant and UV–vis absorption spectra were recorded over time. Compound **1**(o) shows a reversible reduction at −2.11 V, so the potential was held at −2.35 V to ensure reduction occurred. Fig. 13 (left) shows the absorption spectral changes during electrochemical reduction of **1**(o). The resulting spectrum exhibits an absorption maximum at 521 nm as seen in Fig. 13 (left). This is consistent with the ring-closing observed from **1**(o) to **1**(c) via irradiation which gives rise to a new absorption band centred at 531 nm, so we propose that this reduction event leads to a ring closing to give [**1**(c)]•− similar to what has been previously reported for related fulgide switches.[55] The calculated SOMO of [**1**(o)]•− (Fig. 14a) illustrates how this electrochemically induced ring closing mimics the photoinduced ring closing. Population of the LUMO of **1**(o) gives a virtually identical SOMO with antibonding character at the CC double bonds involved which facilitates conrotatory ring closing as shown in Fig. 14b to give [**1**(o)]•−.
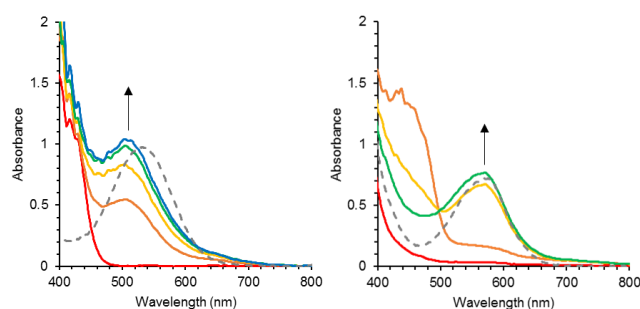
Fig. 13. UV-vis spectra recorded during controlled-potential coulometry (−2.35 V vs. Fc/Fc+) of a 1 mM solution 298 K of **1**(o) in CH₃CN containing 0.1 M Bu₄NPF₆. Dashed grey line is a 25.0 μM solution of **1**(c) in methanol scaled for comparison to spectroelectrochemical spectra (left) and **1**(o) in CH₃CN containing 0.1 M Bu₄NPF₆. Dashed grey line is a 0.1 mM solution of **2**(o) in CH₃CN scaled for comparison to spectroelectrochemical spectra (right).
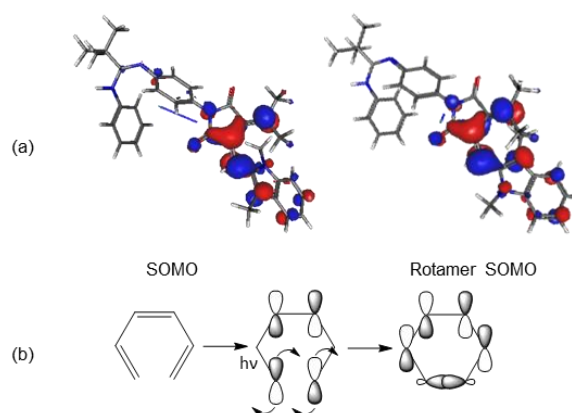
Fig. 14. (a) SOMO of [**1**(o)]•− and its rotamer (shown for clarification, 0.04 a.u. isosurfaces). (b) Conrotatory ring-closing mechanism for both **1**(o) → **1**(c) and [**1**(o)]•− → [**1**(c)]•−.

Compound **2**(c) undergoes a quasi-reversible oxidation at –0.08 V, so the potential was held at 0.20 V to ensure oxidation occurred. Fig. 13, right, shows the changes to the absorption spectrum during electrochemical oxidation of **2**(c). A new peak is observed at 575 nm comparable to the new absorption band at 537 nm that appears upon thermal or photochemical ring opening. This is consistent with oxidation and concomitant ring opening to give [**2**(o)]$^{\bullet+}$ in acetonitrile (Fig. S34). Previous studies have proposed this type of electrochemically induced ring opening of spiropyrans.[51,58,63] Oxidative C-C coupling can occur at the position that is para to the indoline nitrogen when that position is unsubstituted,[56] but that position is substituted in **2** so no coupling is expected.

Given that irradiation induces a measurable change in the redox properties of the carboxamidine group, the possibility that photoisomerisation can influence the redox properties of a coordinated metal seem likely. Preliminary efforts to form isolable coordination complexes with either **1** or **2** have not yet been successful. Metalation strategies for these ligands are being actively explored. To aid this, the non-switchable aryl and alkyl groups can be modified to tune the solubility and crystallinity of the desired complexes, without changing the photoswitchable behaviour.

Conclusions

Two carboxamidine molecules with integrated photoswitchable groups have been prepared on multi-gram scales. In both cases the photoswitchable behaviour of the parent compound is maintained. Good thermal stability is observed for the fulgimide-modified carboxamidine (showing no thermal switching at or above room temperature) and reasonable thermal stability (taking 11 hours to reach thermal equilibrium at 303 K) is observed for the spiropyran-modified carboxamidine. Both molecules are electrochemically active; isomerisation can be induced by reduction of the fulgimide or oxidation of the spiropyran. The oxidation potential of the carboxamidine group changes in response to the light-induced switching of the pendant group. In the case of the fulgimide it becomes easier to oxidize while switching the spiropyran form to the merocyanine form causes the carboxamidine group to become harder to oxidize. This is consistent with DFT calculations that show that switching the fulgimide from open to closed pushes electron density towards the carboxamidine while switching the spiropyran to the merocyanine pulls electron density away from the carboxamidine. This suggests that the photoinduced switching of the pendant group can be used to modulate the ligand field of the corresponding amidinate when bound to a metal. Considering the good agreement between calculations and the experimental results, DFT should be a reliable tool in the design of new systems that show larger changes at the ligating group upon isomerisation of a pendant photoswitch.

Acknowledgements

Notes and references

1   R. Zheng, X. Mei, Z. Lin, Y. Zhao, W. Lv and Q. Ling, Strong CIE activity, multi-stimuli-responsive fluorescence and data storage application of new diphenyl maleimide derivatives, *J. Mater. Chem. C*, 2015, **3**, 10242–10248.
2   L. Hu, Y. Duan, Z. Xu, J. Yuan, Y. Dong and T. Han, Stimuli-responsive fluorophores with aggregation-induced emission: implication for dual-channel optical data storage, *J. Mater. Chem. C*, 2016, **4**, 5334–5341.
3   H. Gao, Y. Bi, J. Chen, L. Peng, K. Wen, P. Ji, W. Ren, X. Li, N. Zhang, J. Gao, Z. Chai and Y. Hu, Near-Infrared Light-Triggered Switchable Nanoparticles for Targeted Chemo/Photothermal Cancer Therapy, *ACS Appl. Mater. Interfaces*, 2016, **8**, 15103–15112.
4   X. An, A. Zhu, H. Luo, H. Ke, H. Chen and Y. Zhao, Rational Design of Multi-Stimuli-Responsive Nanoparticles for Precise Cancer Therapy, *ACS Nano*, 2016, **10**, 5947–5958.
5   L. Zhang and L. Chen, Fluorescence Probe Based on Hybrid Mesoporous Silica/Quantum Dot/Molecularly Imprinted Polymer for Detection of Tetracycline, *ACS Appl. Mater. Interfaces*, 2016, **8**, 16248–16256.
6   A. M. Lifschitz, R. M. Young, J. Mendez-Arroyo, C. M. McGuirk, M. R. Wasielewski and C. A. Mirkin, Cooperative Electronic and Structural Regulation in a Bioinspired Allosteric Photoredox Catalyst, *Inorg. Chem.*, 2016, **55**, 8301–8308.
7   S. Sun, X. Yu, Y. Guo, L. Chen, X. Wang and Z. Jiang, Temperature-Responsive Polyoxometalate Catalysts for DBT Desulfurization in One-Pot Oxidation Combined with Extraction, *Catal. Surv. Asia*, 2016, **20**, 98–108.
8   Y. Nakabayashi and Y. Nosaka, OH Radical Formation at Distinct Faces of Rutile TiO2 Crystal in the Procedure of Photoelectrochemical Water Oxidation, *J. Phys. Chem. C*, 2013, **117**, 23832–23839.
9   Á. Valdés, Z.-W. Qu, G.-J. Kroes, J. Rossmeisl and J. K. Nørskov, Oxidation and Photo-Oxidation of Water on TiO$_2$ Surface, *J. Phys. Chem. C*, 2008, **112**, 9872–9879.
10 Z. Ding, G. Q. Lu and P. F. Greenfield, Role of the Crystallite Phase of TiO$_2$ in Heterogeneous Photocatalysis for Phenol Oxidation in Water, *J. Phys. Chem. B*, 2000, **104**, 4815–4820.
11 E. Krausz and J. Ferguson, in *Progress in Inorganic Chemistry*, ed. S. J. Lippard, John Wiley & Sons, Inc., 1989, pp. 293–390.
12 B. M. Neilson and C. W. Bielawski, Illuminating Photoswitchable Catalysis, *ACS Catal.*, 2013, **3**, 1874–1885.
13 M. Vlatković, B. S. L. Collins and B. L. Feringa, Dynamic Responsive Systems for Catalytic Function, *Chem. – Eur. J.*, 2016, **22**, 17080–17111.
14 D. Bléger and S. Hecht, Visible-Light-Activated Molecular Switches, *Angew. Chem. Int. Ed.*, 2015, **54**, 11338–11349.
15 B. M. Neilson, V. M. Lynch and C. W. Bielawski, Photoswitchable N-Heterocyclic Carbenes: Using Light to Modulate Electron-Donating Properties, *Angew. Chem. Int. Ed.*, 2011, **50**, 10322–10326.
16 B. M. Neilson and C. W. Bielawski, Photoswitchable Metal-Mediated Catalysis: Remotely Tuned Alkene and Alkyne Hydroborations, *Organometallics*, 2013, **32**, 3121–3128.
17 B. M. Neilson and C. W. Bielawski, Photoswitchable Organocatalysis: Using Light To Modulate the Catalytic Activities of N-Heterocyclic Carbenes, *J. Am. Chem. Soc.*, 2012, **134**, 12693–12699.

18 M. M. Paquette, B. O. Patrick and N. L. Frank, Determining the Magnitude and Direction of Photoinduced Ligand Field Switching in Photochromic Metal–Organic Complexes: Molybdenum–Tetracarbonyl Spirooxazine Complexes, *J. Am. Chem. Soc.*, 2011, **133**, 10081–10093.

19 R. A. Kopelman, S. M. Snyder and N. L. Frank, Tunable Photochromism of Spirooxazines via Metal Coordination, *J. Am. Chem. Soc.*, 2003, **125**, 13684–13685.

20 R. A. Kopelman, M. M. Paquette and N. L. Frank, Photoprocesses and magnetic behavior of photochromic transition metal indoline[phenanthrolinospirooxazine] complexes: Tunable photochromic materials, *Inorganica Chim. Acta*, 2008, **361**, 3570–3576.

21 M. M. Paquette, R. A. Kopelman, E. Beitler and N. L. Frank, Incorporating optical bistability into a magnetically bistable system: a photochromic redox isomeric complex, *Chem. Commun.*, 2009, 5424–5426.

22 M. Nihei, Y. Suzuki, N. Kimura, Y. Kera and H. Oshio, Bidirectional Photomagnetic Conversions in a Spin-Crossover Complex with a Diarylethene Moiety, *Chem. – Eur. J.*, 2013, **19**, 6946–6949.

23 M. Milek, F. W. Heinemann and M. M. Khusniyarov, Spin Crossover Meets Diarylethenes: Efficient Photoswitching of Magnetic Properties in Solution at Room Temperature, *Inorg. Chem.*, 2013, **52**, 11585–11592.

24 C. Roux, J. Zarembowitch, B. Gallois, T. Granier and R. Claude, Toward Ligand-Driven Light-Induced Spin Changing. Influence of the Configuration of 4-Styrylpyridine (stpy) on the Magnetic Properties of Fe^{II}(stpy)$_4$(NCS)$_2$ Complexes. Crystal Structures of the Spin-Crossover Species Fe(trans-stpy)$_4$(NCS)$_2$ and of the High-Spin Species Fe(cis-stpy)$_4$(NCS)$_2$, *Inorg. Chem.*, 1994, **33**, 2273–2279.

25 F. T. Edelmann, in *Advances in Organometallic Chemistry*, ed. A. F. H. and M. J. Fink, Academic Press, 2008, vol. 57, pp. 183–352.

26 J. Barker and M. Kilner, The coordination chemistry of the amidine ligand, *Coord. Chem. Rev.*, 1994, **133**, 219–300.

27 Y. Yokoyama, Fulgides for Memories and Switches, *Chem. Rev.*, 2000, **100**, 1717–1740.

28 G. Berkovic, V. Krongauz and V. Weiss, Spiropyrans and Spirooxazines for Memories and Switches, *Chem. Rev.*, 2000, **100**, 1741–1754.

29 P. H. M. Budzelaar, A. B. van Oort and A. G. Orpen, β-Diiminato Complexes of V^{III} and Ti^{III} – Formation and Structure of Stable Paramagnetic Dialkylmetal Compounds, *Eur. J. Inorg. Chem.*, 1998, **1998**, 1485–1494.

30 Y. Liang, A. S. Dvornikov and P. M. Rentzepis, Photochemistry of photochromic 2-indolylfulgides with substituents at the 1′-position of the indolylmethylene moiety, *J. Photochem. Photobiol. Chem.*, 2001, **146**, 83–93.

31 E. I. Balmond, B. K. Tautges, A. L. Faulkner, V. W. Or, B. M. Hodur, J. T. Shaw and A. Y. Louie, Comparative Evaluation of Substituent Effect on the Photochromic Properties of Spiropyrans and Spirooxazines, *J. Org. Chem.*, 2016, **81**, 8744–8758.

32 C. J. Roxburgh, P. G. Sammes and A. Abdullah, Steric and electronically biasing substituent effects on the Photoreversibility of novel, 3′-, 5′- and 3-substituted indolospirobenzopyrans. Thermal evaluation using 1H NMR spectroscopy and Overhauser enhancement studies, *Dyes Pigments*, 2009, **83**, 31–50.

33 H. Görner, Photochromism of nitrospiropyrans: effects of structure, solvent and temperature, *Phys. Chem. Chem. Phys.*, 2001, **3**, 416–423.

34 A. K. Chibisov and H. Görner, Photochromism of spirobenzopyranindolines and spironaphthopyranindolines, *Phys. Chem. Chem. Phys.*, 2001, **3**, 424–431.

35 Y. Sheng, J. Leszczynski, A. A. Garcia, R. Rosario, D. Gust and J. Springer, Comprehensive Theoretical Study of the Conversion Reactions of Spiropyrans: Substituent and Solvent Effects, *J. Phys. Chem. B*, 2004, **108**, 16233–16243.

36 G. Tomasello, M. J. Bearpark, M. A. Robb, G. Orlandi and M. Garavelli, Significance of a Zwitterionic State for Fulgide Photochromism: Implications for the Design of Mimics, *Angew. Chem. Int. Ed.*, 2010, **49**, 2913–2916.

37 S. Uchida, S. Yamada, Y. Yokoyama and Y. Kurita, Steric Effects of Substituents on the Photochromism of Indolylfulgides, *Bull. Chem. Soc. Jpn.*, 1995, **68**, 1677–1682.

38 S. Uchida, Y. Yokoyama, J. Kiji, T. Okano and H. Kitamura, Electronic Effects of Substituents on Indole Nitrogen on the Photochromic Properties of Indolylfulgides, *Bull. Chem. Soc. Jpn.*, 1995, **68**, 2961–2967.

39 R. Chindam, H. M. Hoque, A. S. Ali, F. Z. Rafique and J. D. Gough, Theoretical assessment of indolylfulgimides and novel asymmetric di-indolylfulgimide photochromes, *J. Photochem. Photobiol. Chem.*, 2014, **279**, 38–46.

40 Y. Liang, A. S. Dvornikov and P. M. Rentzepis, Synthesis of novel photochromic fluorescing 2-indolylfulgimides, *Tetrahedron Lett.*, 1999, **40**, 8067–8069.

41 J. Andréasson, S. D. Straight, T. A. Moore, A. L. Moore and D. Gust, Molecular All-Photonic Encoder–Decoder, *J. Am. Chem. Soc.*, 2008, **130**, 11122–11128.

42 A. S. Dvornikov, Y. Liang, C. S. Cruse and P. M. Rentzepis, Spectroscopy and Kinetics of a Molecular Memory with Nondestructive Readout for Use in 2D and 3D Storage Systems, *J. Phys. Chem. B*, 2004, **108**, 8652–8658.

43 L. Li, F.-Q. Bai, J. Wang and H.-X. Zhang, Theoretical investigation on the spectroscopy prosperities of four isomers of an encoder molecule FGDTE, *Dyes Pigments*, 2014, **107**, 108–117.

44 Y. Liang, A. S. Dvornikov and P. M. Rentzepis, Synthesis of novel photochromic fluorescing 2-indolylfulgimides, *Tetrahedron Lett.*, 1999, **40**, 8067–8069.

45 G. Naren, S. Li and J. Andréasson, One-Time Password Generation and Two-Factor Authentication Using Molecules and Light, *ChemPhysChem*, 2017, 1729-1729.

46 P. Remón, M. Bälter, S. Li, J. Andréasson and U. Pischel, An All-Photonic Molecule-Based D Flip-Flop, *J. Am. Chem. Soc.*, 2011, **133**, 20742–20745.

47 A. Abdullah, T. G. Nevell, P. G. Sammes and C. J. Roxburgh, Unusual thermo(photo)chromic properties of some mononitro- and dinitro- substituted 3′-alkyl indolospirobenzopyrans, *Dyes Pigments*, 2015, **121**, 57–72.

48 N. Sivasankaran and K. Palaninathan, Photochromic switchable pendant indolyl fulgimide polypyrrole, *Polym. Degrad. Stab.*, 2013, **98**, 1852–1861.

49 J. T. C. Wojtyk, A. Wasey, P. M. Kazmaier, S. Hoz and E. Buncel, Thermal Reversion Mechanism of N-Functionalized Merocyanines to Spiropyrans: A Solvatochromic, Solvatokinetic, and Semiempirical Study, *J. Phys. Chem. A*, 2000, **104**, 9046–9055.

50 A. K. Chibisov and H. Görner, Complexes of spiropyran-derived merocyanines with metal ions: relaxation kinetics, photochemistry and solvent effects, *Chem. Phys.*, 1998, **237**, 425–442.

51 M. Zanoni, S. Coleman, K. J. Fraser, R. Byrne, K. Wagner, S. Gambhir, D. L. Officer, G. G. Wallace and D. Diamond, Physicochemical study of spiropyran–terthiophene derivatives: photochemistry and thermodynamics, *Phys. Chem. Chem. Phys.*, 2012, **14**, 9112–9120.

52 Y. Shiraishi, K. Yamamoto, S. Sumiya and T. Hirai, Spiropyran as a reusable chemosensor for selective colorimetric detection of aromatic thiols, *Phys. Chem. Chem. Phys.*, 2014, **16**, 12137–12142.

53 B. Daoust and J. Lessard, Electrochemical behavior of amidine hydrochlorides and amidines, *Can. J. Chem.*, 1995, **73**, 362–374.

54 H. E. Abdou, A. A. Mohamed and J. P. Fackler, Synthesis, Characterization, Luminescence, and Electrochemistry of New Tetranuclear Gold(I) Amidinate Clusters: $Au_4[PhNC(Ph)NPh]_4$, $Au_4[PhNC(CH_3)NPh]_4$, and $Au_4[ArNC(H)NAr]_4$, *J. Clust. Sci.*, 2007, **18**, 630–641.

55 M. A. Fox and J. R. Hurst, Electrochemically induced pericyclic reactions. A radical anionic cyclization, *J. Am. Chem. Soc.*, 1984, **106**, 7626–7627.

56 O. Ivashenko, J. T. van Herpt, P. Rudolf, B. L. Feringa and W. R. Browne, Oxidative electrochemical aryl C–C coupling of spiropyrans, *Chem. Commun.*, 2013, **49**, 6737–6739.

57 M. Campredon, G. Giusti, R. Guglielmetti, A. Samat, G. Gronchi, A. Alberti and M. Benaglia, Radical ions and germyloxyaminoxyls from nitrospiro[indoline-naphthopyrans]. A combined electrochemical and EPR study, *J. Chem. Soc. Perkin Trans. 2*, 1993, 2089–2094.

58 G. Armendáriz-Vidales, E. Martínez-González, D. Hernández-Melo, J. Tiburcio and C. Frontana, Electrochemical Characterization of Spiropyran Structures, *Procedia Chem.*, 2014, **12**, 41–46.

59 J. A. Mata, F. E. Hahn and E. Peris, Heterometallic complexes, tandem catalysis and catalytic cooperativity, *Chem. Sci.*, 2014, **5**, 1723–1732.

60 T. Hirao, Conjugated systems composed of transition metals and redox-active π-conjugated ligands, *Coord. Chem. Rev.*, 2002, **226**, 81–91.

61 A. M. Allgeier and C. A. Mirkin, Ligand Design for Electrochemically Controlling Stoichiometric and Catalytic Reactivity of Transition Metals, *Angew. Chem. Int. Ed.*, 1998, **37**, 894–908.

62 V. Lyaskovskyy and B. de Bruin, Redox Non-Innocent Ligands: Versatile New Tools to Control Catalytic Reactions, *ACS Catal.*, 2012, **2**, 270–279.

63 M. J. Preigh, M. T. Stauffer, F.-T. Lin and S. G. Weber, Anodic oxidation mechanism of a spiropyran, *J. Chem. Soc. Faraday Trans.*, 1996, **92**, 3991–3996.
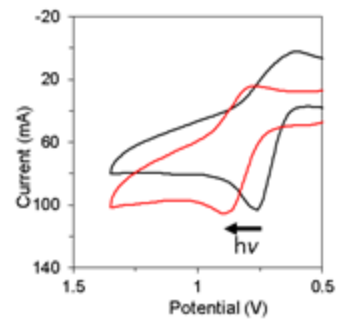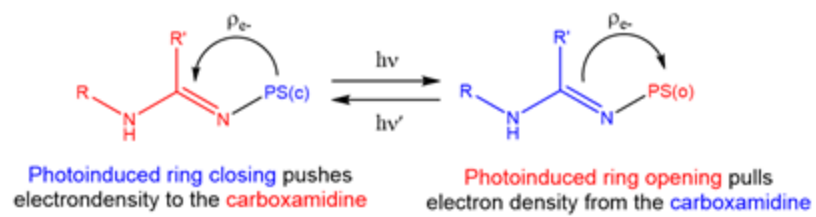
Photo-induced isomerization of a spiropyran or fulgimide results in a measurable change in the electronic structure of a pendant carboxamidine.